Exploring the neuroprotective mechanism of poly-ICLC preconditioning against oxygen glucose deprivation in the *in vitro* blood-brain barrier model

by

Claire B. Turina

A PROJECT

submitted to

Oregon State University

University Honors College

in partial fulfillment of
the requirements for the
degree of

Honors Baccalaureate of Science in Biochemistry and Biophysics

Presented May 13, 2014
Commencement June 2014

AN ABSTRACT OF THE THESIS OF

Claire B. Turina for the degree of Honors Baccalaureate of Science in Biochemistry & Biophysics presented on May 13, 2014. Title: Exploring the neuroprotective mechanism of poly-ICLC preconditioning against oxygen-glucose deprivation in the *in vitro* blood-brain barrier model.

Abstract Approved: _____
Dr. Indira Rajagopal

The preconditioning agent poly-ICLC has recently been shown to protect against cerebral injury in the mouse model, when administered systemically prior to ischemic insult. However, the mechanism by which poly-ICLC provides neuroprotection is currently unknown, but it has been shown to protect against ischemia-induced blood-brain barrier (BBB) disruption. Inflammation contributes to BBB disruption through the vascular changes that promote leukocyte transmigration into ischemic tissue. Vascular cell adhesion molecule-1 (VCAM-1) is the predominant leukocyte trafficker across the BBB during the inflammatory response. This research was aimed at investigating the effect of poly-ICLC preconditioning on VCAM-1 expression at the BBB in response to ischemia. The effect of poly-ICLC preconditioning on the expression of VCAM-1 at the BBB was assessed using an *in vitro* BBB model comprised of primary murine brain microvascular endothelial cells (BMECs) and mixed glial cells co-cultured in a transwell system. Oxygen-glucose deprivation (OGD) served as the *in vitro* model for ischemia. Results from this study showed that BMECs and mixed glial cells upregulate VCAM-1 in response to poly-ICLC preconditioning stimuli.

Key Words: ischemia, vascular cell adhesion molecule-1 (VCAM-1), blood-brain barrier (BBB), poly-ICLC, preconditioning
Corresponding email address: turinac@onid.oregonstate.edu

Exploring the neuroprotective mechanism of poly-ICLC preconditioning against oxygen glucose deprivation in the *in vitro* blood-brain barrier model

by

Claire B. Turina

A PROJECT

submitted to

Oregon State University

University Honors College

in partial fulfillment of
the requirements for the
degree of

Honors Baccalaureate of Science in Biochemistry and Biophysics (Honors Associate)

Presented May 13, 2014
Commencement June 2014

Honors Baccalaureate of Science in Biochemistry & Biophysics project of Claire B. Turina presented on May 13, 2014

APPROVED:

_____

Dr. Indira Rajagopal, Mentor, representing Biochemistry & Biophysics

_____

Dr. Keri Vartanian, Committee Member, representing Oregon Health & Science University

_____

Dr. Viviana Perez, Committee Member, representing Linus Pauling Institute

_____

Dr. Toni Doolen, Dean, University Honors College

I understand that my project will become part of the permanent collection of Oregon State University, University Honors College. My signature below authorizes release of my project to any reader upon request.

_____

Claire B. Turina, Author

ACKNOWLEDGEMENTS

I would like to extend my sincere thanks to Dr. Mary Stenzel-Poore for her mentorship and the amazing opportunity to work in her lab. Also, I am deeply indebted to Dr. Indira Rajagopal, my major advisor, for her guidance and encouragement throughout my undergraduate studies. I extend my appreciation to Dr. Keri Vartanian for her mentorship, advice, and patience throughout my thesis project. I would also like to acknowledge Dr. Viviana Perez for her assistance and advice with my thesis project. Thank you as well to Kyle Haggerty for her help in performing the experiments as well as all the members of Dr. Mary Stenzel-Poore's lab for passing along their research expertise and for their willingness to assist me throughout my experiments. Thank you Sadie, Kelsey, Taylor, Maggie, Sarah, and all of my friends for your moral support. Lastly, I am very grateful to my mother, Mary, my father, John, and my brothers, Christopher and Nicholas for their continued support and encouragement throughout my college studies at Oregon State University.

TABLE OF CONTENTS

LIST OF FIGURES

LIST OF APPENDIX FIGURES

LIST OF ABBREVIATIONS

Toll-like receptors	TLRs
Polyinosinic polycytidylic acid	Poly-IC
Polyinosinic polycytidylic acid carboxymethylcellulose poly-L-lysine	Poly-ICLC
Toll-like receptor-3	TLR3
Blood-brain barrier	BBB
Cell adhesion molecules	CAMs
Vascular cell adhesion molecule-1	VCAM-1
Brain microvascular endothelial cells	BMECs
Oxygen glucose deprivation	OGD
Trans-endothelial electrical resistance	TEER
Quantitative polymerase chain reaction	qPCR
Dulbecco's modified Eagle medium	DMEM
Fetal bovine serum	FBS
Lipopolysaccharide	LPS
Immunohistochemical	IHC

With love, this thesis is dedicated to my family and friends.

Exploring the neuroprotective mechanism of poly-ICLC preconditioning against oxygen glucose deprivation in the *in vitro* blood-brain barrier model

Introduction

Ischemic stroke

Stroke is a leading cause of serious long-term disability and mortality in the United States with approximately 795,000 people experiencing a new or recurrent stroke each year. Ischemic strokes account for 87% of the total number of strokes each year (1). During an ischemic stroke, the blood supply to a region of the brain is disrupted due to a blood clot or atherosclerotic plaque obstructing the blood vessel (2). The cognitive and neurological effects of a stroke are dependent on the size and location of the affected region of the brain, referred to as infarct volume, and the duration of the blockage. Patients undergoing cardiac surgery are at an elevated risk of having perioperative or postoperative ischemic lesions. Postoperative tests have revealed that between 25 and 50% of patients undergoing cardiac surgery develop new ischemic lesions, with a greater occurrence of postoperative lesions in lengthier surgeries (3). Despite the extensive need for an effective antecedent therapy for surgically induced ischemic stroke, there is currently no such treatment.

Preconditioning

A promising therapeutic approach to prevent ischemic damage is preconditioning. Preconditioning is defined as the exposure to a harmful stimulus that is below the threshold for tissue injury, but confers protection against a subsequent, more severe insult

(4). It is known that the evolutionarily conserved Toll-like receptors (TLRs) are integral mediators of tissue injury in response to ischemic stroke. Tissue injury activates TLRs causing them to initiate a robust inflammatory response that can increase tissue damage. However, TLRs also have the ability to self-regulate and develop tolerance. Prior exposure to low-level TLR activation reprograms the TLR pathways, inducing protection against subsequent, more severe insults. In the context of cerebral ischemic damage, TLR tolerance leads to decreased infarct volume and improved neurological outcomes by an enhanced interferon response. TLR preconditioning has been identified as a potential antecedent therapy for patients at a high risk of experiencing a stroke (5).

Poly-ICLC preconditioning

Polyinosinic polycytidylic acid (poly-IC) has been identified as a preconditioning agent that could protect against ischemic stroke. Poly-IC is a synthetic double stranded RNA that has been shown to activate a complex immune response (6). Unfortunately, poly-IC failed in preclinical trials because it was rapidly inactivated by enzymes in the blood (7). Poly-ICLC is a stabilized version of poly-IC with added poly-L-lysine and carboxymethylcellulose moieties to improve pharmacokinetics (6). Poly-ICLC is a clinical-stage therapeutic being evaluated for multiple uses including vaccines, multiple sclerosis, cancer, and viral infections. Preconditioning with poly-ICLC is a promising antecedent treatment to reduce perioperative and postoperative ischemic damage. Poly-ICLC has been shown to protect against cerebral ischemic damage in both the *in vitro* model of ischemic injury and the *in vivo* experimental mouse model of stroke (6,4). Poly-ICLC also has a low risk of toxicity and does not induce a robust inflammatory response,

unlike related therapies. The mechanism by which poly-ICLC confers neuroprotection is currently unknown, though it has been suggested that it works through type-1 interferon signaling (6). Understanding the mechanism by which poly-ICLC confers neuroprotection could lead to the development of a therapeutic to prevent acute ischemic damage.

Blood-brain barrier (BBB)

One of the suggested mechanisms for poly-ICLC ischemic protection is that it reduces damage to the brain parenchyma by preventing the harmful blood-brain barrier (BBB) disruption, which often accompanies a stroke (8). The BBB is a selectively permeable barrier formed by microvascular endothelial cells connected to one another by tight junctions and astrocytic endfeet (Figure 1).

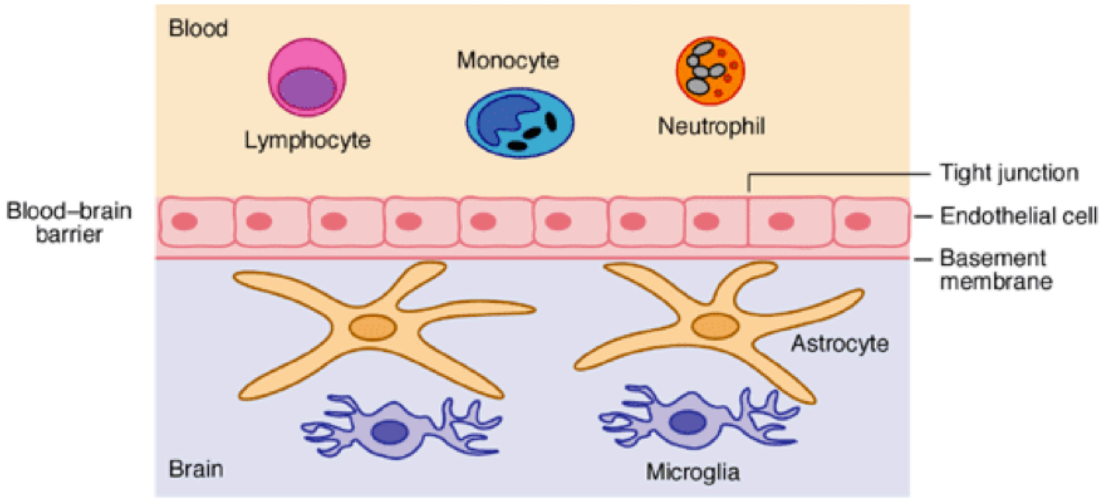

Figure 1: Blood-brain barrier (BBB).
The BBB consists of endothelial cells joined together by tight junctions on the vascular side and astrocytic endfeet in the brain parenchyma. The BBB shields susceptible neurons from the damaging inflammatory cells or leukocytes (lymphocytes, monocytes, and neutrophils), which are constantly circulating in the blood.

The BBB serves a two-fold function. The first function is to shield the susceptible neurons from the potentially toxic substances and immune cells circulating in the blood. Secondly, the BBB functions as a homeostatic mechanism that ensures a constant supply of nutrients and oxygen to the brain (9). Neighboring neurovascular units, formed by the microvascular endothelial cells and astrocytic endfeet, allow cellular communication not only along the BBB, but also with the connected neurons and axons (10).

Ischemia-induced BBB disruption

BBB disruption is one of the first events during the onset of ischemic injury, and it is associated with an increased infarct volume and decreased neurological scoring. This disruption is characterized by an increase in the selective permeability of the BBB due to the loss of tight junction integrity (4). The ischemic consequences to BBB disruption can be permanent or transient depending on the severity of the ischemic insult. BBB disruption is partially a result of the inflammatory response, which causes endothelial cell swelling, astrocyte detachment, and blood vessel rupture in the ischemic region. The recruitment of leukocytes to the ischemic area and their subsequent transmigration across the BBB into ischemic tissue contributes to the increase in vascular activation that is observed during stroke (10).

Inflammatory response to ischemic injury

The inflammatory response is the body's biological reaction to tissue damage through the instigation of protective and restorative mechanisms. Stroke is associated with a chronic inflammatory response, which can exacerbate tissue injury. However, anti-

inflammatory drugs have not proven to be an effective clinical approach to improving stroke outcome. This indicates that the inflammatory response is not entirely detrimental and has some regenerative and restorative effects that without which the clinical outcome is worse (10).

A key component of the inflammatory response is the recruitment and infiltration of leukocytes into the damaged tissue. Leukocytes are recruited to the ischemic area through a series of adhesive events culminating in their transmigration through the BBB into ischemic brain tissue. Diapedesis is the process by which a leukocyte moves through tight endothelial cell borders or through the endothelial cell body (11). Diapedesis takes place *via* three highly regulated steps. Selectin molecules are responsible for regulating the first step, which is referred to as "rolling." Circulating leukocytes are temporarily captured *via* cell-to-cell interactions with the selectins along the microvascular endothelium. Cell adhesion molecules (CAMs) regulate the second step, "adhesion," characterized by the firm sticking of leukocytes to the surface of the endothelium. The leukocyte then crawls along the endothelium through tightly regulated integrin/CAM-mediated interactions until it reaches a site for optimal transmigration. The final step is the transmigration of the leukocyte through, or between, the endothelial cells. Transmigration is also regulated by the CAMs and the chemokine-signaling cascade, allowing the leukocyte to penetrate and travel through the BBB into ischemic brain tissue. Ischemic injury causes upregulation of the expression of molecules involved in diapedesis (12). The excessive infiltration of leukocytes into the brain is typically associated with increased cerebral inflammation as well as a worsened stroke outcome (13). It has been proposed that poly-

ICLC confers neuroprotection against ischemia by mediating the expression of molecules directly involved in diapedesis.

The CAMs are members of the immunoglobin superfamily. They are responsible for the activation and firm adherence of leukocytes to the blood vessel wall and the facilitation of their subsequent extravasation across the BBB into ischemic tissue. CAMs are constitutively expressed along the cell membrane of endothelial cells, leukocytes, epithelial cells, and fibroblasts (10). Under physiological conditions, CAMs serve a protective role, but under ischemic conditions they contribute to the inflammatory response through the increased firm adhesion and extravasation of leukocytes, which leads to BBB disruption and secondary injury to the brain (8).

Vascular cell adhesion molecule-1

Vascular cell adhesion molecule-1 (VCAM-1) is a major regulator of the migration of leukocytes along the vascular endothelium and their transmigration through the BBB (13). VCAM-1firmly binds to monocytes and lymphocytes with the CD49/CD29 integrin receptors. VCAM-1 clustering along the vascular endothelium occurs as the leukocyte is approaching the ischemic region. This clustering stimulates an increase in cytosolic free calcium ions and reactive oxygen species, which are known to cause weakening of the endothelial tight junctions and promote leukocyte transmigration (11). Through stimulating the weakening of tight junctions, VCAM-1 is directly contributing to the increases in BBB permeability associated with increased damage to the brain parenchyma.

Both human and *in vitro* studies investigating the effect of ischemic conditions on VCAM-1 expression have shown upregulation of VCAM-1 on BMECs following ischemic stress (8,14). It is thought that this increase in VCAM-1 expression enables increased leukocyte activation and adhesion causing secondary tissue damage to previously salvageable cells. Poly-ICLC may protect the BBB integrity by decreasing perivascular inflammation through downregulating the expression of cell adhesion molecules such as VCAM-1. This downregulation of VCAM-1 would result in decreased leukocyte invasion of ischemic tissue. It was hypothesized that poly-ICLC preconditioning would attenuate the ischemia-induced upregulation of VCAM-1. This research project aims to investigate the effect of poly-ICLC preconditioning on the *in vitro* expression of VCAM-1 on primary murine brain microvascular endothelial cells (BMECs) and mixed glial cells following ischemic insult.

Materials and Methods

Study Design

The effect of poly-ICLC preconditioning on VCAM-1 expression in response to ischemia was investigated using an *in vitro* BBB model. The *in vitro* BBB model consists of primary murine brain microvascular endothelial cell (BMECs) and mixed astrocytes and microglia co-cultured in a transwell system (Figure 2). The *in vitro* model for ischemia consists of 5h of oxygen-glucose deprivation (OGD) followed by 24h of reoxygenation. Cells were treated with poly-ICLC for 24h and all treatments were removed prior to OGD.

Trans-endothelial electrical resistance (TEER) and permeability measurements were used to test for protection against ischemia-induced BBB disruption. TEER measurements assess the integrity of the tight junctions of the endothelial cell monolayer, and permeability measurements assess the alterations in transcellular and paracellular transport. TEER measurements were taken immediately before and after OGD, as well as, 24h following OGD. Permeability measurements were obtained 24h following OGD. qPCR and protein expression analyses were performed 24h following OGD. To investigate the effect of poly-ICLC preconditioning alone, cells were treated with poly-ICLC for 24h, medium was then changed, and 24h later VCAM-1 expression was analyzed. VCAM-1 expression was analyzed using qPCR, immunohistochemical staining, and Western blot quantitation.

Drug treatments

Primary cells were treated in both compartments of the co-culture dish with either fresh medium or poly-ICLC (2 μg/mL) in fresh medium 24h prior to OGD, and all treatments were removed prior to OGD.

***in vitro* BBB model**

Primary cultures of mixed glial cells and astrocytes were prepared from the brains of 1-2 day postnatal mice. The mice were sacrificed and their brains collected. The meninges were removed and cortical pieces were homogenized and incubated for 15 min at 37 ºC with trypsin (2.5 mg/mL: Invitrogen. Grand Island. NY. USA) and DNAse I (0.08 mg/mL: Sigma). Supernatant was collected, centrifuged, and resuspended in Dulbecco's modified Eagle medium (DMEM, Invitrogen) containing 0.5 mg/mL gentamicin (Sigma) and 10% FBS. The cells were cultured on poly-$_{L}$-lysine (Sigma) coated 12-well plates 3 weeks prior to the experiment (4).

Brain microvascular endothelial cells (BMECs) were prepared from 8-12 week-old male mice. Mice were sacrificed and the forebrains were collected and meninges removed in ice-cold sterile phosphate buffered saline (PBS). The gray matter was minced into 1 mm^3 pieces and digested with 1 mg/mL collagenase CLS2 (Worthington. Lakewood. NJ, USA) in DMEM for 45 min at 37 ºC. The microvessels were separated from the myelin-containing components by centrifugation at 1000g, for 20 min in 20% bovine serum albumin (BSA: Sigma) in DMEM. The microvessels were further digested to remove pericytes from the basal membrane with 1 mg/mL collagenase-dispase (Roche, Mannheim, Germany) in DMEM for 30 min. A 33% continuous Percoll gradient

(Amersham, Piscataway, NJ, USA) was used to separate microvascular endothelial cell clusters. The cells were collected and seeded on collagen type IV and fibronectin coated cell culture inserts (Transwell clear, 1.12 cm^2: pore size. 0.4 µm. Costar. Lowell, MA. USA). Cultures were grown in DMEM supplemented with 5 µg/mL gentamicin (Sigma), 20% plasma-derived bovine serum (First Link. Wolverhamptom, UK), 200 µg/mL endothelial cell growth supplement (Sigma), and 100 µg/mL heparin (Sigma). During the first two days of culture, the culture medium contained 4 µg/mL puromycin (Sigma) to selectively remove P-glycoprotein negative cells. Cultures reached confluency within 4-5 days (4).

To simulate the BBB, murine BMECs were co-cultured with mixed mouse cerebral astrocytes and microglia cells. The BMEC-containing transwell inserts were placed into multiwell plates with the mixed glial cells in the bottom compartment and medium was replaced with fresh endothelial cell culture medium two days after seeding. Twenty-four hours after co-culture the culture medium was supplemented with 250 µM 8-(4-Chlorophenylthio)adenosine 3',5'-cyclic monophosphate sodium salt (CPT-cAMP) (Sigma) and 17.5 µM 4-(3-Butoxy-4-methoxybenzyl)imidiazolidin-2-one (RO 201724) (Sigma) for 24h to tighten the tight junctions and elevate monolayer resistance (4).

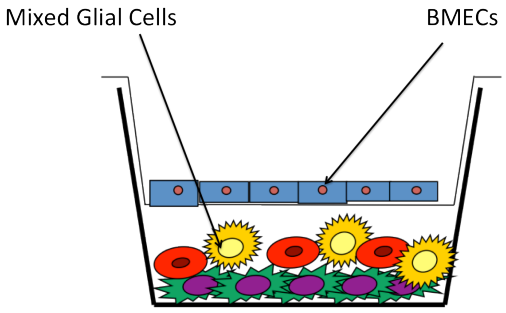

Figure 2: The *in vitro* blood-brain barrier (BBB) model.
The *in vitro* BBB model consists of brain microvascular endothelial cells (BMECs) and mixed glial cells co-cultured in a transwell system.

Measurement of monolayer resistance

Trans-endothelial electrical resistance (TEER) was measured using an EVOM resistance meter (World Precision Instruments. Sarasota, FL, USA) using STX-2 electrodes. Resistance was expressed in units of the surface area of the endothelial monolayer (cm^2). The TEER of the cell-free inserts (80-90 cm^2) was subtracted from the measurements. TEER measurements were taken immediately prior to OGD, immediately following OGD, and 24h post OGD (4).

Permeability measurements

Paraceullar transport was assessed by measuring the flux of Na-fluorescein (Sigma), and transcellular transport was determined by measuring the flux of peroxidase-conjugated albumin (Jackson ImmunoResearch, West Grove, PA, USA). BMEC cultures were transferred to 12-well plates containing 1.5 mL/well of DMEM without phenol red and endothelial cells were washed with DMEM without phenol red. After the phenol red was sufficiently removed, 500 μL of DMEM without phenol red containing 10 μg/mL Na-fluorescein (MW = 376 Da) and 0.5 μg/mL of peroxide albumin (MW = 67 kDa) was applied to the cell cultures. Cells were placed on an agitator (90-100 rpm) in a 37 °C incubator. At 15, 30, 60, 120, and 240 min the inserts were transferred to a new well containing 1.5 mL/well of DMEM without phenol red. Flux across cell-free inserts was also determined at those time points. The concentrations of Na-fluorescein and peroxidase-conjugated albumin were determined in the samples obtained from the lower compartments. Marker molecule concentrations were measured using a plate reader (Spectra Max 190, absorbance 450 nm for Albumin and Spectra Max Gemini XS

emission: 515 nm, excitation 460 nm for Na-fluorescein; Molecular Devices, Sunnyvale, CA, USA). Measurements were analyzed as described in Gesuete *et al*.

Oxygen-glucose deprivation (OGD)

BMECs and glial cell co-cultures were incubated in a hypoxic chamber for 5h and culture medium was replaced with deoxygenated glucose-free medium. The anaerobic atmosphere of the hypoxic chamber, which consisted of 85% N_2, 10% CO_2, and 5% H_2, was monitored using an electronic oxygen/hydrogen analyzer (Coy Laboratories, Grass Lake, MI, USA). After 5h of OGD, medium was replaced with normoglycemic medium and co-cultures were returned to a normoxic incubator for 24h reoxygenation. In the control co-culture, medium was replaced with fresh complete culture medium and the co-culture was not exposed to OGD conditions (4).

RNA isolation, reverse transcription, and quantitative PCR

RNA was isolated from individual BMEC or glial cell wells at 24h and 48h following poly-ICLC treatment and 24h after OGD using the Mini RNA isolation kit (Qiagen, Valencia, CA, USA). DNAse treatment was performed on 1 μg of RNA using Turbo DNAse treatment (Life Technologies, Grand Island, NY, USA). RNA was reverse transcribed using the High Capacity cDNA Reverse Transcription kit (Life Technologies). Quantitative PCR (qPCR) was performed using Taqman Gene Expression Assays (Applied Biosystems) for each gene of interest on the StepOne Plus qPCR machine (Applied Biosystems). Results were normalized to β-actin expression and

analyzed relative to their control counterparts. The relative quantification of VCAM-1 expression was carried out using the comparative CT method ($2^{-\Delta\Delta ct}$).

Immunohistochemical analysis of VCAM-1 expression

BMECs, 24h post-poly-ICLC treatment and 24h post-OGD, adhered to transwell membrane, were fixed with ice-cold ethanol for 30 min at 4°C. Glial cells plated on glass, 24h following poly-ICLC treatment and 24h post OGD, were fixed with 1% formalin for 15 min at room temperature. Cells were washed with dPBS prior to 30 min incubation at room temperature with 1% Triton for permeabilization followed by 30 min with 3% FBS in PBS for blocking. The cells were incubated with the primary antibody, rabbit monoclonal Anti-VCAM-1 (1:400, EPR5047. Abcam. Cambridge, United Kingdom) in 3% FBS in PBS overnight at 4°C. Cells were then washed three times with dPBS prior to application of goat-anti rabbit IgG-HRP rabbit polyclonal IgG secondary antibody (1:1000, sc-2004 Lot #A2313. Santa-Cruz Biotech. Santa Cruz, CA, USA) for 1h 30 min at room temperature on agitator (60 rpm). Cells were mounted on glass slides using mounting solution that contained the DAPI stain. IHC images were acquired using the Olympus BX61 microscope equipped with an Olympus confocal scan unit FV1000 (Olympus, Hicksville, NY, USA) and visualized using ImageJ (FIJI. Madison, WI, USA).

Quantitation of VCAM-1 expression using Western blot analysis

Protein was isolated using Trizol® protocol (ThermoFisher Scientific. Waltham, MA, USA) and protein concentrations were determined using Pierce® BCA Assay (ThermoFisher Scientific). Due to low protein concentrations, the maximum amount of

protein was denatured at 95°C for 5 min and then loaded into a gel and ran at 150 V for 1h 15 min. Protein was then transferred to a PVDF membrane for 3h at 75 V. The membrane was then blocked in 5% milk blocking solution for 1h prior to application of the rabbit monoclonal anti-VCAM-1 primary antibody (1: 1000; EPR5047 Abcam. Cambridge, United Kingdom) in 2% milk blocking solution overnight at 4° C. The membrane was washed three times with 1X PBST prior to application of goat anti-rabbit secondary antibody (1:10,000, IgG-HRP, sc-2004 Lot #A2313. Santa-Cruz Biotech. Santa Cruz, CA, USA) in 2% milk blocking solution for 1h at room temperature. The membrane was washed three times with 1X PBST and then equal parts of ECL substrate and enhancer solution were applied to the blot for 1 min and then the blot was imaged. To normalize the amount of protein loaded in each lane, the membrane was stripped and reacted with actin antibody (1:1000, rabbit polyclonal IgG I-19-R, sc-1616-R lot #1006. Santa-Cruz Biotech. Santa Cruz, CA, USA) in 2% blocking solution overnight at 4° C. The blot was washed with PBST and the secondary antibody (1:10,000, IgG-HRP, sc-2004 Lot #A2313. Santa-Cruz Biotech. Santa Cruz, CA, USA) was applied for 1h on agitator (70 rpm). VCAM-1 and actin blots were analyzed using FIJI software to measure the density of the bands. The density of the VCAM-1 band was normalized to the intensity of the actin band to determine the relative amount of VCAM-1 per sample.

Statistical analysis

Data are represented by average ± SD. Statistical analysis was performed on combined experiments using GraphPad Prism5 software (La Jolla, CA, USA). One-way Anova with

Tukey *post hoc* test for gene expression analysis. p-values that were less than 0.05 were considered to be statistically significant.

Results

Poly-ICLC preconditioning attenuates OGD-induced BBB disruption

The integrity of the BBB model was assessed prior to OGD, immediately following OGD, and 24h post OGD. Trans-endothelial electrical resistance (TEER), paracellular transport, and transcellular transport measurements were obtained to characterize the BBB model and to assess protection against OGD. After four days of co-culture, control BMECs showed high TEER values and low endothelial permeability coefficients for Na fluorescein (paracellular) and albumin (transcellular) transport (Figure 3). Prior work from the lab has shown that the observed values are consistent with the accepted values for a murine *in vitro* BBB model and are considered representative of a functional murine BBB (4).

A significant decrease in TEER was observed immediately following OGD compared to control co-cultures, and no recovery was observed 24h post OGD. However, the poly-ICLC preconditioned co-cultures showed an attenuated drop in TEER immediately following OGD compared to the untreated OGD co-cultures. Additionally, a slight recovery of TEER was observed 24h following OGD (Figure 3a). OGD caused drastic increases in both the paracellular and transcellular transport 24h post OGD (Figure 3c). Poly-ICLC preconditioned cells maintained transport coefficient values similar to those of the control cells. These results suggest that poly-ICLC preconditioning protects the *in vitro* BBB model by attenuating the ischemia-induced decrease in TEER and by maintaining basal levels of BMEC permeability despite OGD.

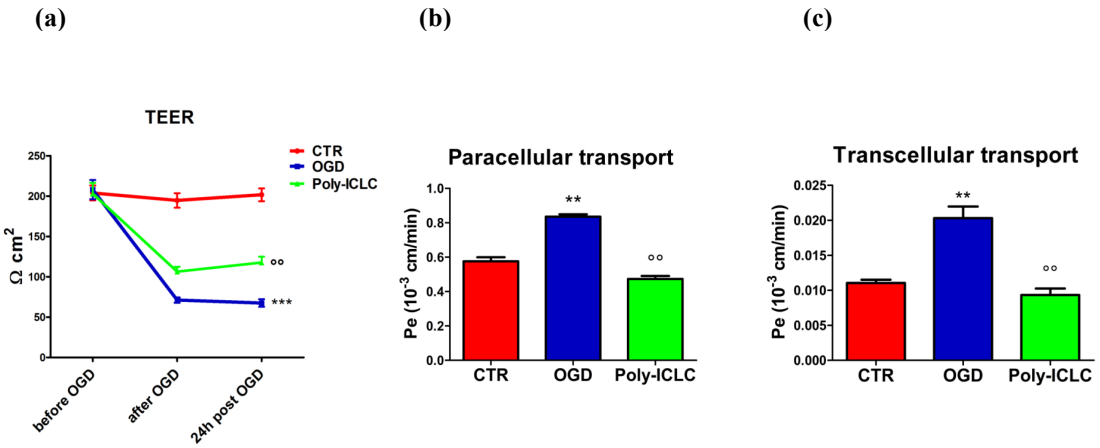

Figure 3: Poly-ICLC preconditioning protects the *in vitro* BBB model (4)
(a) Trans-endothelial electrical resistance (TEER) values of the co-cultured BMECs obtained prior to OGD, immediately following OGD, and 24h post OGD. Control co-cultures were unexposed to any experimental conditions, but both OGD and poly-ICLC preconditioned co-cultures underwent 5h OGD. *** $p < 0.05$ versus control and °° $p < 0.05$ versus OGD. **(b)** Paracellular transport permeability coefficient (Pe) values measured using Na-fluorescein reporter molecule 24h post OGD. ** $p < 0.05$ versus control and °° $p < 0.05$ versus OGD**. (c)** Transcellular transport Pe values measured using the albumin reporter molecule 24h post OGD. ** $p < 0.05$ versus control and °° $p < 0.05$ versus OGD.

Poly-ICLC preconditioned cells showed a trend toward upregulation of VCAM-1 expression

To evaluate the effect of poly-ICLC preconditioning on VCAM-1 expression at the BBB, qPCR was performed on both the BMECs and glial cells under various experimental conditions. qPCR analysis on the BMECs 24h after OGD showed that OGD did not consistently elevate VCAM-1 expression. However, VCAM-1 was consistently upregulated in poly-ICLC preconditioned BMECs that were exposed to OGD (Figure 4a). OGD did not affect glial cell VCAM-1 expression, but poly-ICLC preconditioned glial cells showed a statistically significant increase in VCAM-1 expression after OGD when compared to the experimental control (Figure 4b).

Based on the variable effect OGD had on VCAM-1 expression, further investigation was done to determine whether poly-ICLC preconditioning alone was increasing

VCAM-1 expression. Two additional time points were considered, 24h and 48h following poly-ICLC treatment, and the cells were not exposed to OGD. The BMECs showed a trend toward upregulation of VCAM-1 24h post-treatment compared to the experimental control. But 48h post-treatment, VCAM-1 expression on BMECs was downregulated when compared to the expression at 24h post-treatment and to the experimental control (Figure 4a). The glial cells showed statistically significant upregulation of VCAM-1 expression 24 and 48h following poly-ICLC treatment compared to the experimental control (Figure 4b).

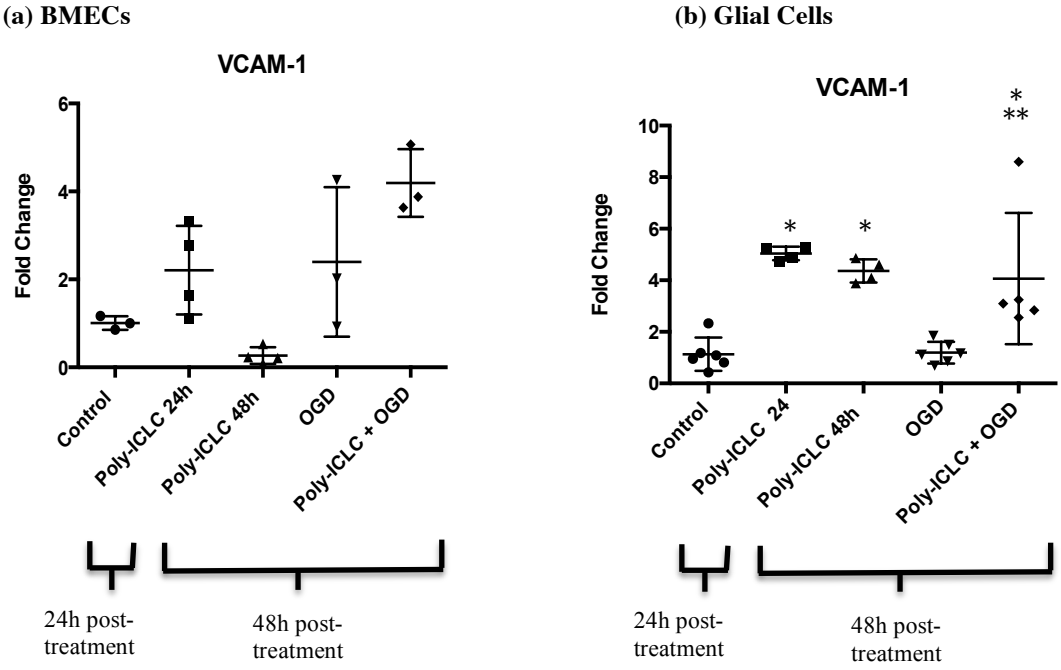

Figure 4: VCAM-1 gene expression is upregulated following poly-ICLC preconditioning
(a) qPCR analysis on BMECs from the *in vitro* BBB model. Cells were treated with 2 μg/mL poly-ICLC 24h prior to undergoing 5h of OGD; RNA was isolated 24h following OGD. To analyze the effect of poly-ICLC alone on cells, RNA was isolated 24h and 48h after treatment. **(b)** qPCR analysis on glial cells from the *in vitro* BBB model. *$p < 0.05$ compared to control group; **$p < 0.05$ compared to OGD group

Some of the variability seen in the BMEC experiments is likely due to the low RNA yield obtained during isolation. Therefore, the amount of RNA used for the reverse transcription and qPCR experiments was not ideal. This resulted in some of the values being extremely close to the threshold. Additional RNA isolation protocols were tested in an attempt to increase RNA yield, but these methods were also unsuccessful. Based on this consideration, we decided to look at VCAM-1 protein expression using IHC staining and Western blot analysis.

Immunohistochemical staining showed regulation of VCAM-1 expression on poly-ICLC preconditioned BMECs

Immunohistochemical (IHC) staining was used to evaluate protein expression and spatial location. Control BMECs from the *in vitro* BBB model showed very little constitutive VCAM-1 expression on control BMECs. VCAM-1 expression on BMECs was induced by OGD, but this upregulation was attenuated in poly-ICLC preconditioned cells (Figure 5a). However, in a second experiment, more constitutive VCAM-1 expression was observed on the control cells. VCAM-1 was slightly upregulated in both the poly-ICLC preconditioned and untreated cells 24h after OGD. No attenuation of the OGD-induced VCAM-1 expression was observed in the poly-ICLC preconditioned cells (Figure 5b).

(a)

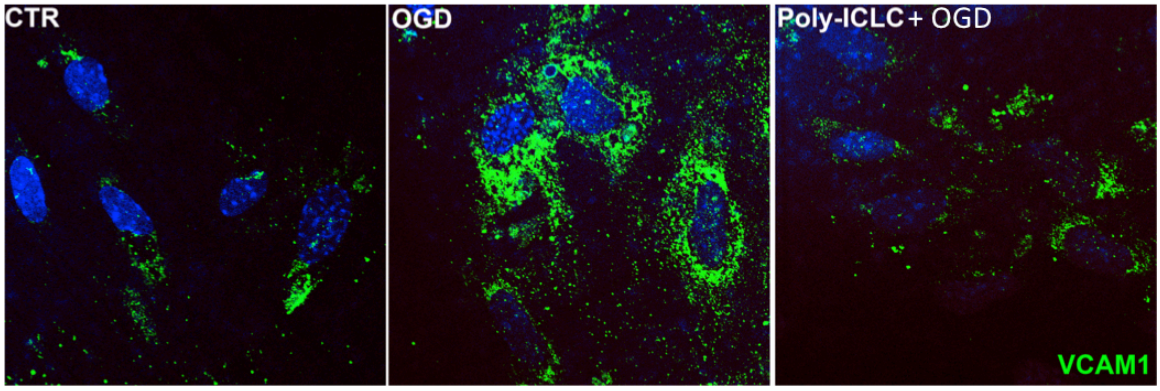

(b)

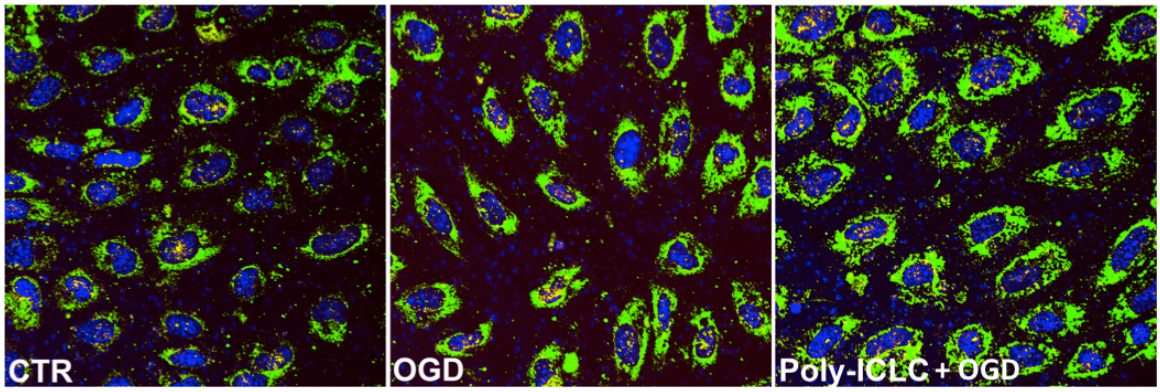

Figure 5: IHC staining of BMECs showed variable VCAM-1 expression depending on experiment **(a)** IHC staining of BMECs from the first experiment 24h following OGD. DAPI was used to stain cell nuclei while FITC was used to identify VCAM-1. Control cells were untreated and were not exposed to OGD. OGD cells were only exposed to OGD and poly-ICLC cells were treated with poly-ICLC 24h prior to 5h of OGD. (**b)** IHC staining of BMECs from the second experiment. Cells were exposed to the same experimental conditions as the first experiment and the same staining protocol was followed.

Based on the results from the BMEC qPCR experiments, we were interested in investigating the effect of poly-ICLC preconditioning alone on BMEC VCAM-1 expression. The BMECs were preconditioned with poly-ICLC 24h prior to fixation. This time point was selected for this study because it was when the cells in previous experiments were exposed to OGD. This isolated any changes in VCAM-1 expression that occurred prior to OGD. Results showed minimal baseline expression of VCAM-1 on

the control cells, and a dramatic upregulation of VCAM-1 expression on the poly-ICLC preconditioned BMECs (Figure 6). These results indicate that VCAM-1 is upregulated in poly-ICLC preconditioned BMECs prior to ischemic exposure.

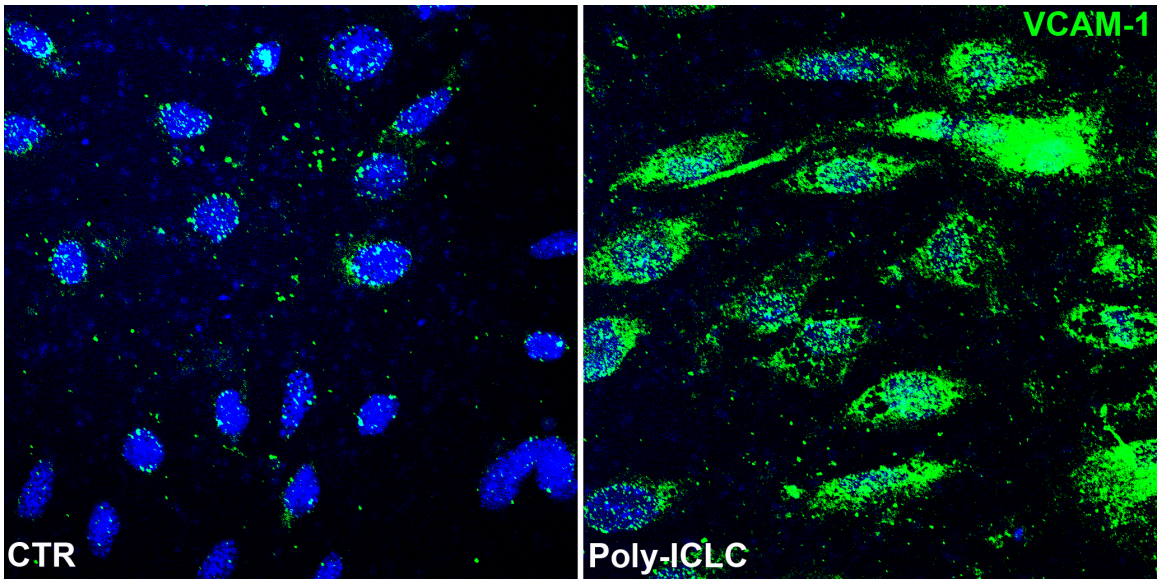

Figure 6: IHC staining on poly-ICLC preconditioned BMECs unexposed to OGD showed upregulation of VCAM-1 expression.
IHC staining of primary BMECs 24h post treatment. Images represent untreated (control) or poly-ICLC (2 μg/mL) treated BMECs at 24h post-treatment. DAPI was used to stain cell nuclei while FITC was used to identify VCAM-1.

IHC staining showed regulation of VCAM-1 expression on poly-ICLC preconditioned glial cells

IHC staining was also performed on the glial cells plated on glass that were not co-cultured with BMECs due to experimental constraints. Results showed no constitutive expression of VCAM-1 on the glial cells. OGD induced a slight upregulation of VCAM-1 expression on the glial cells. The expression of VCAM-1 was the same in the preconditioned glial cells that were also exposed to OGD as it was in the cells exposed to OGD alone. This indicates that poly-ICLC preconditioning did not affect VCAM-1 expression in response to OGD. However, there is an upregulation of VCAM-1

expression in the cells that were exposed to only poly-ICLC and this upregulation is greater than that seen in the OGD and poly-ICLC+OGD samples. These results are supported by an additional experiment, shown in Figure 8, in which glial cells plated on glass and not co-cultured with BMECs were given poly-ICLC preconditioning at the same dose for 24h and then fixed.

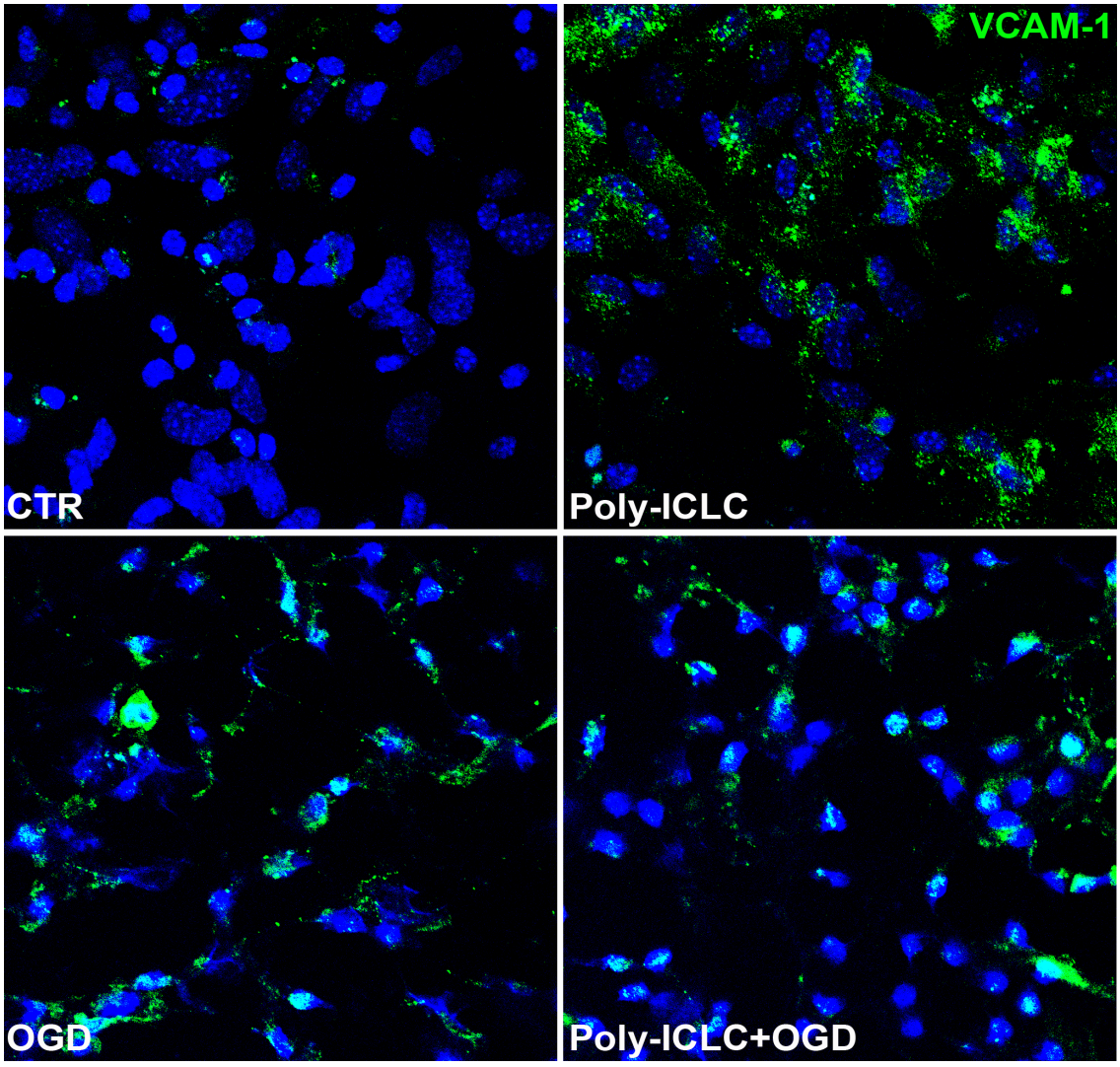

Figure 7: IHC staining on the primary glial cells showed upregulation of VCAM-1 on poly-ICLC preconditioned cells.
IHC staining was performed on glial cells that were plated on glass with an empty transwell membrane insert in the top chamber. Cells were treated with 2 μg/mL poly-ICLC or fresh media 24h prior to OGD. The control and poly-ICLC cells were given fresh media at the time of OGD, while the OGD and poly-ICLC+OGD cells were exposed to 5h OGD. Cells were fixed 24h following OGD. DAPI was used to stain cell nuclei and FITC was used to identify VCAM-1.

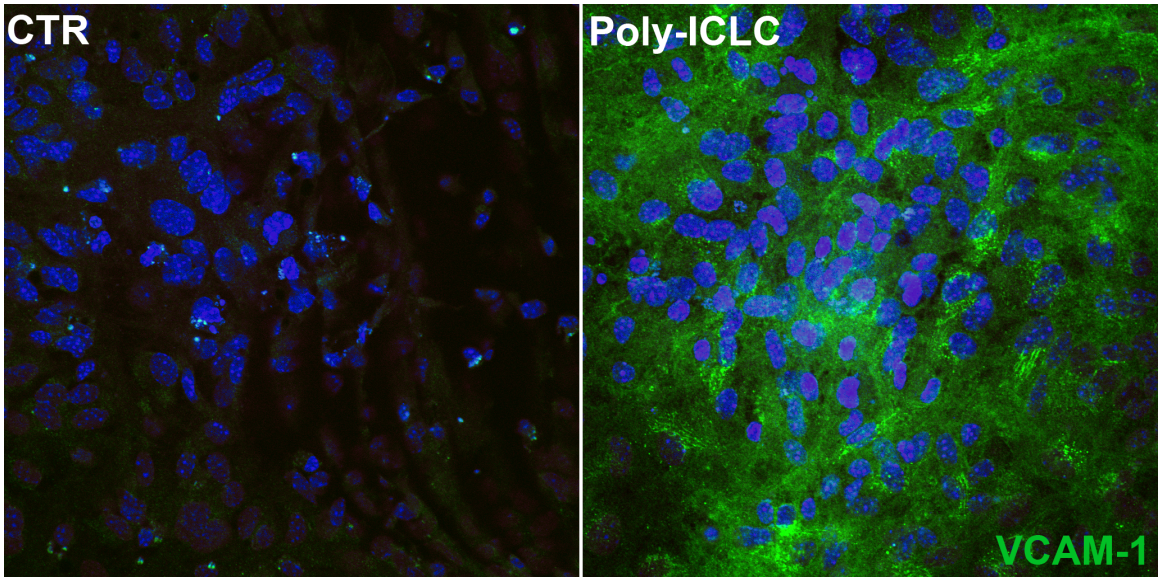

Figure 8: Poly-ICLC preconditioned glial cells upregulate VCAM-1 expression in the absence of ischemic exposure.
IHC staining of primary glial cells 24h post treatment. Control cells were untreated, but poly-ICLC cells were treated with 2 μg/mL for 24h.

VCAM-1 protein expression is upregulated in poly-ICLC preconditioned cells

Since the results from the qPCR and protein expression experiments were variable, additional methods were considered that would allow the isolation of both RNA and protein from the same sample. In previous experiments, RNA isolation and IHC staining could only be performed on samples from different wells. Trizol was utilized to isolate protein and RNA from the same well, thereby limiting the well-to-well variability. Prior to isolation of experimental samples, a test experiment was done to compare the RNA and protein that were obtained using the RNeasy and Trizol isolation kits to ensure that the results are comparable. The results from the test experiment showed nearly identical qPCR results and Western blot results from the samples obtained using the two different protocols, indicating that the different isolation methods yielded the same results (Appendix). Previously isolated protein from LPS-treated bEnd.3 cells was used as a

positive control. Protein expression from the positive control was consistent across both the BMEC and glial cell blots and with a previous experiment (Appendix).

Figure 9a shows the Western blot performed on the protein isolated from the glial cells 24h following OGD. VCAM-1 expression was slightly downregulated in untreated cells exposed to OGD; data are supported by qPCR results obtained from the same sample (Figure 9b). VCAM-1 protein expression was upregulated in poly-ICLC preconditioned glial cells that were exposed to OGD. These results also agree with the qPCR data from the same samples.

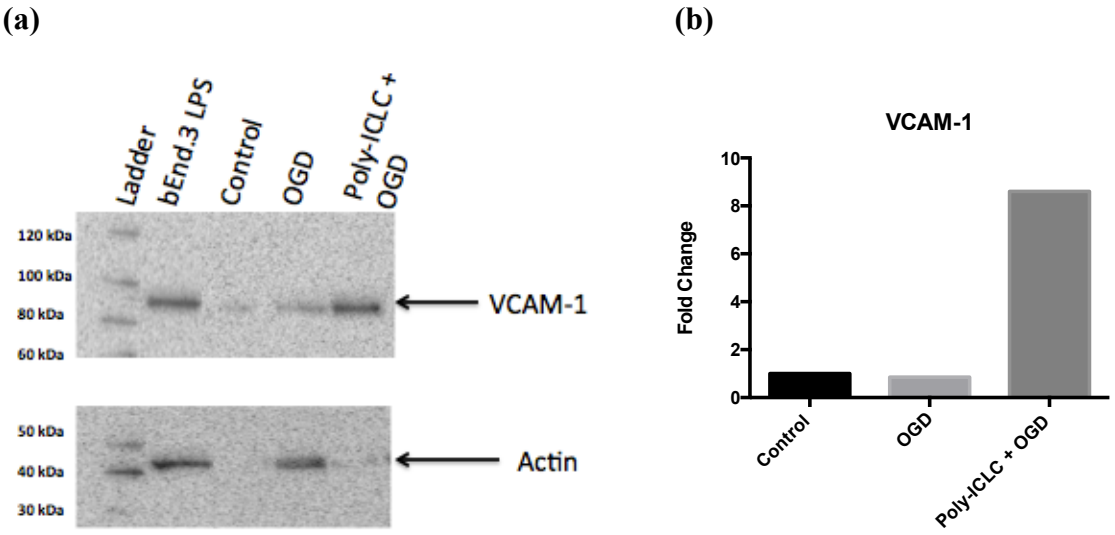

Figure 9: Poly-ICLC preconditioned glial cells upregulate VCAM-1 expression following OGD. **(a)** Western blot data of VCAM-1 expression on glial cells from the *in vitro* BBB model. The maximum amount of protein was loaded in each lane respectively: 34.5 µg, 6.3 µg, 2.9 µg, and 4.6 µg. Protein was isolated 24h following OGD. The bEnd.3. LPS treated sample was used as a positive control. **(b)** qPCR analysis of the same samples.

Results from the Western blot performed on the BMECs from the *in vitro* BBB model are shown in Figure 10a. VCAM-1 protein expression in untreated BMECs exposed to OGD was unreliable due to incomplete protein transfer. Poly-ICLC preconditioned BMECs upregulated VCAM-1 protein expression after OGD exposure. These results are supported by qPCR data obtained from the same well (Figure 10b).

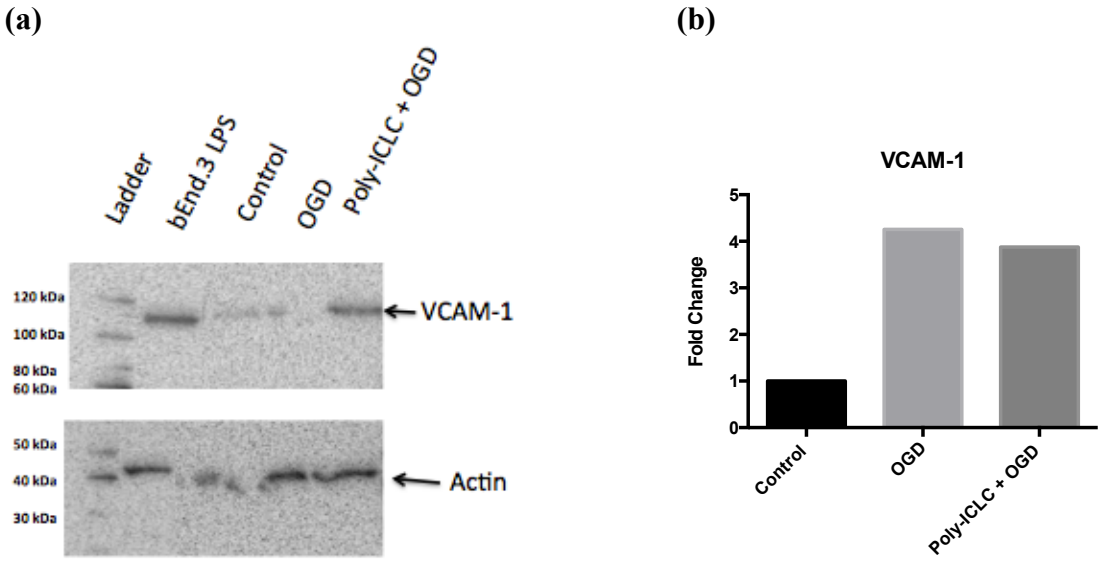

Figure 10: Poly-ICLC preconditioned BMECs upregulate VCAM-1 expression following OGD.
(a) Western blot data of VCAM-1 expression on BMECs from the *in vitro* BBB model. Protein was isolated 24h following OGD and 8.0 μg of protein was loaded in each lane aside from bEnd.3 LPS in which 34.5 μg was loaded. The bEnd.3 LPS treated sample was used as a positive control. **(b)** qPCR analysis of the same samples.

Discussion

Poly-ICLC preconditioned BMECs upregulate VCAM-1 regardless of ischemic-exposure

The purpose of this study was to investigate the effect of poly-ICLC preconditioning on VCAM-1 expression in the *in vitro* BBB model following OGD. I hypothesized that OGD would upregulate VCAM-1 expression on BMECs, and that this increase would be attenuated in poly-ICLC preconditioned cells. However, the results of this study did not support this hypothesis. Instead, qPCR data showed that poly-ICLC preconditioned BMECs upregulated VCAM-1 following OGD, but the effect of OGD alone on VCAM-1 expression was not reproducible. Interestingly, poly-ICLC preconditioning alone had an effect on VCAM-1 expression. In BMECs 24h post-treatment VCAM-1 expression was upregulated. This indicates that, at the time of OGD, the BMECs already upregulated VCAM-1; however, 48h post-treatment VCAM-1 expression was downregulated (Figure 4b). Results from experiments analyzing VCAM-1 protein expression consistently showed VCAM-1 upregulation in poly-ICLC preconditioned BMECs regardless of OGD exposure. Poly-ICLC preconditioned BMECs upregulate VCAM-1 24h post-treatment; this upregulation could be part of the neuroprotective mechanisms of poly-ICLC against cerebral ischemia.

Poly-ICLC preconditioned mixed glial cells also upregulate VCAM-1 regardless of ischemic-exposure

Poly-ICLC preconditioned mixed glial cells also consistently showed upregulation of VCAM-1 prior to OGD. VCAM-1 expression was not affected by OGD alone, but it was upregulated in poly-ICLC preconditioned glial cells that were subsequently exposed to OGD. I did not expect to see regulation of VCAM-1 expression on mixed glial cells

because VCAM-1 is typically associated with the vascular endothelium. However, previous research has shown that VCAM-1 can be expressed on nonvascular cells, including astrocytes (15). VCAM-1 is not expressed on CNS cells under physiological conditions, but VCAM-1 expression can be induced by certain inflammatory cytokines (16). It has also been shown that previous exposure to inflammatory cytokines can influence the outcome of the subsequent cytokine exposure. For instance, Rosenman *et al*. showed that treatment of astrocytes with IFN-γ primes astrocytes to dramatically upregulate VCAM-1 expression upon the subsequent exposure to the IL-1β inflammatory cytokine (15).

The role that VCAM-1 expression plays on astrocytes is currently unclear. Based on the intimate relationship between astrocytes and endothelial cells at the BBB, it is thought that astrocytic expression of VCAM-1 could be a potential mediator of leukocyte trafficking across the BBB. Astrocytic expression of VCAM-1 may also be involved in leukocyte retention within the brain parenchyma (16). VCAM-1 expression on glial cells also may provide important environmental cues for the infiltration of leukocytes into cerebral tissue (15). Also, the influence of previous cytokine exposure on the future expression of VCAM-1 on CNS cells in response to inflammatory cytokines indicates a potential role of astrocytic expression of VCAM-1 in the neuroprotective mechanism of poly-ICLC preconditioning.

Upregulation of VCAM-1 may not correlate with increased tissue damage

The general trend observed was the upregulation of VCAM-1 expression in poly-ICLC preconditioned BMECs and glial cells with and without exposure to OGD. Since it was shown that poly-ICLC protects the *in vitro* BBB against ischemic damage (Figure 2) it is

possible that the upregulation of VCAM-1 expression at the BBB prior to ischemia is part of the neuroprotective mechanism of poly-ICLC preconditioning. Originally, we hypothesized that upregulation of VCAM-1 expression would be associated with a heightened inflammatory response and increased secondary tissue damage. However, results from this study do not support this because VCAM-1 expression is upregulated in poly-ICLC preconditioned cells that are still protected against ischemia. There is evidence that anti-VCAM-1 treatments do not protect *in vivo* against transient ischemic injury. In fact there was a non-significant trend towards increased infarct size and decreased neurological scoring in mice that received the anti-VCAM-1 treatment when compared to the control antibody group (17). These results suggest that elevation of VCAM-1 expression may participate in neuroprotective responses to ischemia.

Upregulation of VCAM-1 prior to ischemic injury could also be associated with initial leukocyte infiltration prior to reperfusion. The presence of leukocytes in the brain prior to ischemic injury may lead to increased neuronal protection against cerebral ischemia. Beck *et al.* observed that the number of activated leukocytes, which are defined as those that are participating in rolling interactions with the BBB cell adhesion molecules, directly correlated with the number of viable neurons following ischemic injury (18). These results suggest that the initial activation of leukocytes could have neuroprotective potential or could indicate ongoing tissue repair. These leukocytes could be involved in immediate repair of damaged, ischemic regions; they could also be involved in preventing ischemic damage.

Conclusions and future research

This research has shown that poly-ICLC preconditioning is upregulating VCAM-1 expression at the BBB prior to ischemic exposure as well as after 24h reperfusion. It is possible that upregulation of VCAM-1 expression is serving a neuroprotective role in poly-ICLC preconditioning. However, further research is need to understand this potential role. This work does establish that poly-ICLC preconditioning does not suppress VCAM-1 expression as was originally hypothesized. This may indicate that VCAM-1 is not involved in the neuroprotection conferred by poly-ICLC preconditioning. To investigate this, anti-VCAM-1 treatments could be administered or VCAM-1 knockout studies could be performed to test whether damage is greater in VCAM-1 deficient cells and mice. It is also possible that different cell adhesion molecules, such as ICAM-1, PECAM-1, or selectins, are involved in poly-ICLC preconditioning. Therefore, similar expression studies should be performed to investigate on other molecules involved in mediating leukocyte trafficking during the inflammatory response to gain more information regarding how poly-ICLC preconditioning mediates the inflammatory response to cerebral ischemia.

However, if VCAM-1 is not involved in the neuroprotective mechanism of poly-ICLC preconditioning, it is unclear why poly-ICLC upregulates VCAM-1 expression. As previously mentioned, there is evidence that anti-VCAM-1 treatments are not protective and that leukocyte infiltration into the brain parenchyma prior to ischemic exposure can increase neuroprotection (17,18). It is possible that VCAM-1 upregulation is part of the neuroprotective mechanism of poly-ICLC preconditioning and that it works through

mediating the initial infiltration of leukocytes across the BBB prior to ischemia. To test this, an *in vitro* leukocyte adhesion assay could be utilized to first see if upregulated expression of VCAM-1 correlates with increased leukocyte adhesion to the microvascular endothelium. Next, two-photon microscopy could be used to visualize the adherence and extravasation of labeled leukocytes *in vivo* through a cranial window. This would allow us to measure the number of leukocytes that attached to the BBB endothelium prior to ischemic exposure. This work has shown that poly-ICLC preconditioning does not downregulate VCAM-1 expression following ischemic exposure, but rather it upregulates VCAM-1 prior to ischemia. Further research is required to understand the role VCAM-1 expression plays in the neuroprotective mechanism of poly-ICLC preconditioning.

REFERENCES

1. Heart disease and stroke statistics—2013 update. Circulation. 2013. January 8;1:132-139.

2. Acute ischemic stroke. Cedars-Sinai. 2014. 1:1-2.

3. Barber P, Gommans J, Fink J, Bennet P, Ataman N. Acute stroke services in New Zealand: changes between 2001 and 2007. N Z Med J. 2008. November 7;121(1285):46-51.

4. Gesuete R, Packard A, Vartanian K, Conrad V, Stevens S, Bahjat F, Yang T, Stenzel-Poore M. Poly-ICLC preconditioning protects the blood-brain barrier against ischemic injury *in vitro* through type I interferon signaling. J Neurochem. 2012. 123(2):75-85.

5. Vartanian K, Stenzel-Poore M. Toll-like receptor tolerance as a mechanism for neuroprotection. Transl Stroke Res. 2010. December 1;1(4):252-260.

6. Packard A, Hedges J, Bahjat F, Stevens S, Conlin M, Salazar A, Stenzel-Poore M. Poly-IC preconditioning protects against cerebral and renal ischemia-reperfusion injury. J Cerebr Blood F Met. 2011. November 16;32:242-247.

7. Salazar A. Activating the natural host defense: Hiltonol (poly-ICLC) and malignant brain tumors. Oncovir Inc. 2013.

8. An P, Xue Y. Effects of preconditioning on tight junction and cell adhesion of cerebral endothelial cells. Brain Res. 2009. 1272:81-88.

9. Ramirez S, Hasko J, Skuba A, Fan S, Dkystra H, McCormick R, Reichenbach N, Krizbai I, Mahadevan A, Zhang M, Tuma R, Son Y, Persidky Y. Activation of cannabinoid receptor 2 attenuates leukocyte-endothelial cell interactions and blood-brain barrier dysfunction under inflammatory conditions. J Neurosci. 2012. March 12;32(12):4004-4016.

10. Ceulemans A, Zgavc T, Kooijman R, Hachimi-Idrissi, Sarre S, Michotte Y. The dual role of the neuroinflammatory response after ischemic stroke: modulatory effects of hypothermia. J Neuroinflamm. 2010. 7(74):1-18.

11. Muller W. Mechanisms of leukocyte transendothelial migration. Annu Rev Pathol Mech Dis. 2011. 6:323-344.

12. Zhou W, Liesz A, Bauer H, Sommer C, Lahrmann B, Valous N, Grabe J, Veltkamp R. Postischemic brain infiltration of leukocyte subpopulations differs among murine permanent and transient focal cerebral ischemia models. Brain Pathol. 2013. 23:34-44.

13. Greenwood J, Heasman S, Alvarez J, Pratt A, Lyck R, Engelhardt B. Leukocyte-endothelial cell crosstalk at the blood-brain barrier: a prerequisite for successful immune cell entry to the brain. Neuropath Appl Neuro. 2011. 37:24-39.

14. Frijins C, Kappelle L. Inflammatory cell adhesion molecules in ischemic cerebrovascular disease. Stroke. 2002. 33:2115-2122.

15. Rosenmann S, Shrikant P, Dubb L, Benveniste E, Ransohoff R. Cytokine-induced expression of vascular cell adhesion molecule-1 (VCAM-1) by astrocytes and astrocytoma cell lines. J Immunol. 1995. 1888-1899.

16. Gimenez M, Sim J, Russel J. TNFR1-dependent VCAM-1 expression by astrocytes exposes the CNS to destructive inflammation. J Neuroimmunol. 2004. 151:116-125.

17. Justicia C, Martin A, Rojas S, Gironella M, Cervera A, Panes J, Chamorrow A, Planas A. Anti-VCAM-1 antibodies did not protect against ischemic damage either in rats or in mice. J of Cerebr Blood F Met. 2006. August. 26:241-432.

18. Beck J, Stummer W, Lehmberg J, Baethmann A, Uhl E. Activation of leuckoyte-endothelial interactions and reduction of selective neuronal death after global cerebral ischemia. Neurosci Lett. 2007. 414:159-164.

APPENDIX

Cell lines

The immortalized bEnd.3 endothelial cell line was used from passages 3-7. The bEnd.3 cells were cultured on 10 cm cell culture dishes in Dulbecco's modified Eagle medium (DMEM: cat. no 30-2002; +L-glut, +glucose, +Na pyruvate, +Na bicarbonate. Invitrogen) supplemented with 10% fetal bovine serum (FBS: HyClone, Austin, TX. USA). The cells were cultured on 12-well plates for the Trizol practice experiment.

bEnd.3 experiment to test Trizol® isolation

bEnd.3 cells were plated on a 12-well tissue culture plate at a seeding density of 2×10^5 cells/well. After one day the cells were confluent and six wells were treated with 1 μg/mL LPS 18h prior to isolation. The Trizol® (ThermoFisher Scientific. Waltham, MA, USA) isolation protocol was performed side by side with the RNeasy mini kit isolation (Qiagen, Valencia, CA, USA) and the whole cell extraction protocol. Reverse transcription and qPCR were used to confirm that the RNA isolated using the Trizol® was consistent with the RNA isolated using the Mini RNA kit. The Pierce® BCA Protein Assay Kit (ThermoFisher Scientific. Waltham, MA, USA) was used to ascertain protein concentration and then Western blot analysis was performed to confirm that the protein isolated using the Trizol® kit was consistent with the protein isolated using the whole cell extraction protocol. The results from this test experiment showed that the Trizol® isolation protocol gave comparable expression data to the RNeasy and whole cell extraction protocols (Appendix Figure 1 and Appendix Figure 2).

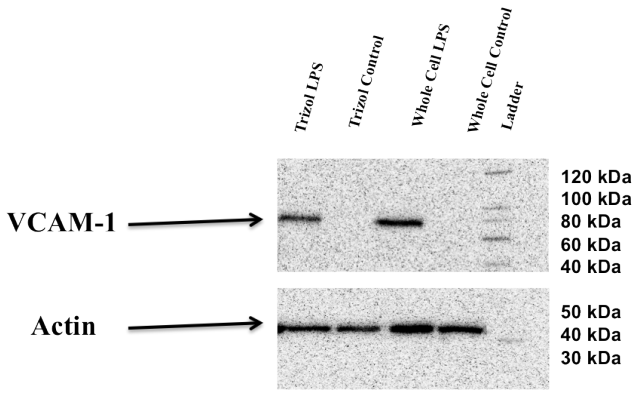

Appendix Figure 1: Trizol® test experiment Western blot
Western blot from protein isolated from the bEnd.3 cells; cells were either treated with 1 μg/mL LPS in culture medium or with new culture medium alone 18h prior to isolation.

Sample	**ΔC_t**	**$\Delta\Delta C_t$**	**Fold Change**
RNeasy Control	10.696		
RNeasy LPS	6.432	-4.262	19.189
Trizol Control	10.764		
Trizol LPS	6.618	-4.146	17.702

Appendix Figure 2: Trizol® test experiment qPCR analysis
qPCR data from RNA isolated from the bEnd.3 cells.